Kinetic temperature and carbon dioxide from broadband infrared limb emission measurements taken from the TIMED/SABER instrument

Christopher J. Mertens [??]

NASA Langley Research Center, 21 Langley Blvd., MS 401B, Hampton, VA 23681-2199, USA

James M. Russell III

Hampton University, 23 Tyler St., Hampton VA 23668, USA

Martin G. Mlynczak

NASA Langley Research Center, 21 Langley Blvd., MS 420, Hampton, VA 23681-2199, USA

Chiao-Yao She

Colorado State University, 200 West Lake St., Fort Collions, CO 80523-1875, USA

Francis J. Schmidlin

NASA Wallops Flight Facility, Code 972, Wallops Island, VA 23337, USA

Richard A. Goldberg

NASA Goddard Space Flight Center, Code 690.4, Greenbelt, MD 20771, USA

Manuel López-Puertas

Instituto de Astrofisica de Andalucia, CSIC, Apdo. 3004, Granada 18080, Spain

Peter P. Wintersteiner

ARCON Corporation, 260 Bear Hill Rd., Waltham, MA 02451, USA

Richard H. Picard and Jeremy R. Winick

Air Force Research Laboratories, Hanscom Air Force Base, Hanscom, MA 01731-3010, USA

Xiaojing Xu

SSAI, Inc., 1 Enterprise Parkway, Hampton VA 23666, USA

Abstract

The Sounding of the Atmosphere using Broadband Emission Radiometry (SABER) experiment is one of four instruments on NASA's Thermosphere-Ionosphere-Energetics and Dynamics (TIMED) satellite. SABER measures broadband infrared limb emission and derives vertical profiles of kinetic temperature (Tk) from the lower stratosphere to approximately 120 km, and vertical profiles of carbon dioxide (CO_2) volume mixing ratio (vmr) from approximately 70 km to 120 km. In this paper we report on SABER Tk/CO_2 data in the mesosphere and lower thermosphere (MLT) region from the version 1.06 dataset. The continuous SABER measurements provide an excellent dataset to understand the evolution and mechanisms responsible for the global two-level structure of the mesopause altitude. SABER MLT Tk comparisons with ground-based sodium lidar and rocket falling sphere Tk measurements

are generally in good agreement. However, SABER CO_2 data differs significantly from TIME-GCM model simulations. Indirect CO_2 validation through SABER-lidar MLT Tk comparisons and SABER-radiation transfer comparisons of nighttime 4.3 μm limb emission suggest the SABER-derived CO_2 data is a better representation of the true atmospheric MLT CO_2 abundance compared to model simulations of CO_2 vmr.

Key words: SABER, temperature, carbon dioxide (CO_2), infrared remote sensing, non-LTE

---

1 Introduction

The Sounding of the Atmosphere using Broadband Emission Radiometry (SABER) experiment was launched onboard the NASA Thermosphere-Ionosphere-Energetics and Dynamics (TIMED) satellite in December 2001 (Russell et al., 1999). SABER is designed to provide measurements of the key radiative and chemical sources and sinks of energy in the mesosphere and lower thermosphere (MLT), in order to achieve major advances in understanding the struc-

* Corresponding author: Tel.: +1 757 864 2179; fax: +1 757 864 6326

Email addresses: `Christopher.J.Mertens@nasa.gov` (Christopher J. Mertens), `james.russell@hamptonu.edu` (James M. Russell III), `Martin.G.Mlynczak@nasa.gov` (Martin G. Mlynczak), `joeshe@lamar.colostate.edu` (Chiao-Yao She), `fjs@osb.wff.nasa.gov` (Francis J. Schmidlin), `Richard.A.Goldberg@nasa.gov` (Richard A. Goldberg), `puertas@iaa.es` (Manuel López-Puertas), `winters@arcon.com` (Peter P. Wintersteiner), `richard.picard@hanscom.af.mil`, `jeremy.winick@hanscom.af.mil` (Richard H. Picard and Jeremy R. Winick), `xiaojing_xu@ssaihq.com` (Xiaojing Xu).

ture, energetics, chemistry, and dynamics of the MLT region from approximately 60 to 180 km. SABER measures Earth limb emission in 10 broadband radiometer channels ranging from 1.27 μm to 17 μm. Measurements are made both day and night over the latitude range from 54° S to 87° N, with alternating hemisphere coverage every 60 days. The continuous sounding of SABER provides ~ 2200 vertical scans of limb radiance per channel per day, which are used to retrieve vertical profiles, with approximately 2 km altitude resolution, of kinetic temperature (Tk), O_3, H_2O, and CO_2 volume mixing ratio (vmr), and volume emission rates from $O_2(^1\Delta)$, OH(v=3-5), OH(v=7-9), and NO(v).

The challenge of deriving the SABER data products is that the MLT infrared emissions are in non-local thermodynamic equilibrium (non-LTE), requiring complex non-LTE radiation transfer algorithms and novel retrieval approaches to derive the key data products. In this paper we report on SABER Tk and CO_2 data, which are retrieved from CO_2 infrared rotation-vibration bands. The results presented in this paper provide a representative assessment of the SABER Tk/CO_2 data products from the version 1.06 dataset and provide a benchmark dataset to compare results of future updates.

2 MLT Kinetic Temperature

During daytime conditions, Tk and CO_2 are retrieved simultaneously from SABER's CO_2 15 μm and CO_2 4.3 μm radiometer channel measurements, respectively (Mertens et al., 2002). During nighttime, Tk is retrieved from the SABER 15 μm channel measurements and the CO_2 concentration is determined from a TIME-GCM climatological database (Mertens et al., 2001; Roble, 1995). In the following two subsections, we summarize SABER MLT

4

results from the version 1.06 dataset.

2.1 Global Characteristics

Figures 1 and 2 are SABER zonal mean averages of MLT Tk for July 2002 and January 2003, respectively. The dashed line in the figures indicate the location of the mesopause height. The two-level structure of the mesopause altitude is evident. For the northern hemisphere summer season shown in Figure 1, the high-altitude mesopause of the southern hemisphere winter season extends into the northern hemisphere before it dramatically transitions to the low-altitude mesopause altitude characteristic of summer conditions. For July 2002, the winter-to-summer transition in mesopause height occurs at 33° N. The average winter (or high) mesopause height is 98 ± 1 km. The average summer (or low) mesopause height is 83 ± 1 km. Note also the extremely low temperatures in the polar summer region were Tk reaches 130 K by 70° N and 128 K at 80° N.

Figure 2 shows the zonal mean average temperature field for the opposite season of Figure 1. In Figure 2, the high-altitude mesopause of the northern hemisphere winter season extends into the southern hemisphere summer season before it dramatically transitions to the low-altitude summer mesopause height. The winter-to-summer mesopause altitude transition occurs at 41° S for January 2003.

The two-level structure of the mesopause altitude is an intriguing feature of the MLT region. Ground-based measurements have observed and characterized the two-level structure of the mesopause at select geographic locations for many years (von Zahn et al., 1996; She and von Zahn, 1998; and references

therein). However, SABER measurements are providing the first continuous global measurements of the MLT thermal structure, an invaluable dataset for understanding the evolution and mechanisms responsible for this striking feature of the MLT region (e.g., Berger and von Zahn, 1999).

2.2   Temperature Comparisons

In this section we present comparisons of SABER MLT Tk with ground-based and in-situ measurements during polar summer conditions. The ability to derive accurate mesospheric Tk from infrared limb emission measurements for polar summer conditions is one of the most stringent tests of the non-LTE Tk/CO_2 retrieval algorithm. Figure 3 shows SABER Tk comparisons with rocket falling sphere (FS) measurements and the Lübken climatological profile for early July (Lübken, 1999). The SABER-FS comparisons were made during the NASA 2002 summer Mountain and Convective Wave Ascending Vertically (MaCWAVE) campaign. The FS measurements were taken at the Andøya rocket range at 69° N, 16° E (Schmidlin et al., 1991). For times of closest coincidence, the SABER-FS Tk differences are within 6 K below 85 km on 2 July and within 6 K below 80 km on 4 July. The SABER results from the non-LTE retrieval algorithm improve retrieved Tk in the mesopause region by 35-45 K as compared to results from the LTE retrievals (i.e., the gray solid lines in Figure 3. Note: The SABER LTE Tk profiles appeared publicly only in an early version of the dataset). The SABER-FS single profile comparisons are generally within $\sim$ 5-10 K below 85 km.

Figure 4 shows SABER Tk comparisons with sodium lidar measurements made during the 2002 summer MaCWAVE campaign. The magnitude of SABER-

6

lidar Tk differences above 90 km are comparable to the SABER-FS Tk differences below 85 km. For the closest time coincidences, the SABER-lidar Tk differences are within 5-10 K between 90-97 km.

Figure 5 shows a comparison of the mean profiles derived from Figures 3 and 4. The horizontal lines are the statistical fluctuations about the mean profile, indicative of natural variability in Tk. The SABER-lidar mean Tk profiles agree within natural variability between 90-95 km on 2 and 4 July, which is $\sim$ 5-10 K. The Tk error in the lidar measurement becomes quite large below 90 km and above 95-97 km, due to the thin sodium layer during polar summer conditions. The SABER-FS mean Tk profiles nearly agree within natural variability below 85 km on 2 July, which is on the order of $\sim$ 5-8 K. However, SABER-FS mean Tk profile differs by more than the estimated natural variability between about 75-85 km on 4 July.

SABER MLT Tk comparisons between ground-based and in-situ measurements during polar summer are generally good below 85 km and between 90-95 km, i.e., within natural variability of the MLT polar summer thermal structure, demonstrating a significant advance in satellite remote sensing of MLT infrared limb emission and the ability to retrieve Tk under extreme non-LTE conditions. The SABER monthly zonal mean mesopause temperature at 69° N for July 2002 is 132 K, which is in excellent agreement with the 129 K mesopause temperature given by the Lübken climatological profile for early July. However, the most noticeable and significant difference between SABER Tk and the FS measurements and the Lübken climatological profile shown in Figures 3-5 are the Tk differences between 85-90 km, due to a $\sim$ 4-5 km difference in mesopause altitude. Mertens et al. (2004) conducted a number of sensitivity studies with respect to key non-LTE and atmospheric input pa-

rameters in order to determine a possible cause for a low mesopause altitude in the non-LTE Tk/CO_2 retrieval algorithm. The non-LTE and atmospheric input parameters included in the study by Mertens et al. were the collisional quenching rate of CO_2 (ν_2) by atomic oxygen, the atomic oxygen concentration, and the CO_2 vmr. The source of CO_2 vmr during the day is from the simultaneous Tk/CO_2 retrieval (Mertens et al., 2002). At night, CO_2 vmr is obtained from a TIME-GCM climatological database (Roble, 1995). The NRLMISIS-00 model is the source of atomic oxygen concentration (Picone et al., 2002). The Sharma and Wintersteiner (1990) rate is used for the nominal CO_2 (ν_2)-O collisional quenching parameter. The conclusion of that study was that the above non-LTE and atmospheric input parameters affect the magnitude of the retrieved Tk, but the change in the location of the mesopause altitude is insignificant.

One way to increase the SABER mesopause altitude is to increase pressure at a lower altitude. For example, absolute pressure-altitude is registered at around 35 km in the LTE Tk retrieval (i.e., $p_o = $ p(z=35 km)) (Remsberg et al., 2004). The pressure profile is built above and below the pressure-altitude registration level (i.e. p_o) using the barometric law. An offset in altitude is approximately related to an error in the pressure-altitude registration by $\delta\,p_o/p_o = \delta\,z/H$. For a 7 km scale height (H = 7 km), an altitude offset of 4 km ($\delta\,z = 4$ km) requires an error in pressure-altitude registration of 57%. This simple relation gives results comparable to a more detailed analysis. Solutions of the hypsometric equation using the SABER Tk profiles from Figures 3 and 4, and perturbing the pressures at 35 km by 60%, increases the location of the mesopause altitude by $\sim$ 3.5 km. Remsberg et al. (2003) compared SABER version 1.01 stratospheric temperature and geopotential height with Met Office

assimilated analysis. They found that the differences are within 2 K for Tk and 160 m for geopotential height. An altitude offset of 160 m corresponds to a $\sim 2.3\%$ error in pressure for a 7 km scale height, which is nearly a factor of 30 less than the pressure-altitude registration error needed to account for a 4 km offset in the SABER mesopause altitude. Thus, uncertainty in the SABER pressure-altitude registration can not account for a 4-5 km offset in the mesopause altitude.

Recent work by Kutepov et al. (2006) partially explains the polar summer Tk mesopause altitude offset of SABER compared to FS measurements and the Lübken climatological profile. By including CO_2 (ν_2) V-V transfer between isotopes, Kutepov et al. showed that the SABER mesopause altitude can be increased by 2-4 km. Moreover, this mechanism will warm SABER Tk by as much as 10-20 K between 75 km and 90 km, bringing the SABER MLT Tk into closer agreement with the FS and Lübken climatological profiles discussed previously. The isotopic CO_2 ν_2 V-V exchange processes will be included in the next version (version 1.07) of the SABER dataset.

Many years of lidar measurements at mid-latitudes have been analyzed to deduce the MLT thermal structure (She et al., 1993, 1995). The summer (or low) mesopause altitude derived from the lidar analysis is 86 ± 3 km. The SABER summer mesopause altitude (83 ± 1 km) agrees with the lidar analysis within statistical fluctuations (natural variability) and the 2 km vertical resolution of the SABER measurement.

In summary, SABER MLT Tk in the polar summer region generally agree with FS and sodium lidar measurements within natural variability. It's anticipated that the incorporation of the isotopic CO_2 (ν_2) V-V exchange processes into

the SABER non-LTE Tk retrieval will reduce the mean systematic differences, such as the mesopause altitude and lower mesospheric Tk, between SABER and the FS measurements and the Lübken climatological profile.

3   MLT CO_2 Concentration

SABER CO_2 vmr is retrieved simultaneously with Tk during the daytime. In the next two subsections we show representative monthly zonal mean SABER-CO_2 data from the version 1.06 dataset and results from our initial validation study.

3.1   Global Characteristics

Monthly zonal mean daytime CO_2 vmr data are shown in Figure 6 for northern hemisphere winter (January 2003), equinox (September 2003), and summer seasons (July 2002). Comparisons of SABER CO_2 vmr with TIME-GCM model data (Roble, 1995) show that CO_2 vmr observed by SABER is systematically lower than the model simulations at altitudes above roughly 70-75 km. This result is consistent with previous CO_2 measurements determined from atmospheric infrared remote sensing observations (Kaufmann et al., 2002; Zaragoza et al., 2000; López-Puertas et al., 2000; and references therein). However, the morphology of the SABER daytime monthly mean CO_2 vmr is generally similar to the TIME-GCM results. The most glaring differences, on the other hand, occur at high-latitude summer seasons (i.e., high-latitude southern hemisphere, January 2003; high-latitude northern hemisphere, July 2002). Specifically, there is a meridional gradient in the SABER CO_2 vmr

10

data near the polar regions not seen in the model data, which increases with season from winter to summer. In fact, there is a step-function feature in the SABER high-latitude summer regions coincident with the latitude region of the auroral oval. This step function feature is seen in the high-latitude southern hemisphere for January 2003 and in the high-latitude northern hemisphere for July 2002.

Simulations and sensitivity studies suggest that $NO^+(v)$ emission at 4.3 μm not accounted for in the non-LTE Tk/CO_2 retrieval algorithm is a plausible explanation for the meridional gradient in the SABER high-latitude summer season CO_2 vmr data. Solar EUV photons ionize the neutral atmospheric constituents, which eventually end up as NO^+ in the ionospheric E-region, due to ion-neutral chemistry. Some of the ion-neutral reactions are exothermic enough to produce vibrationally excited NO^+, which emits at 4.3 μm (Mertens et al., 2007). Not including this emission source in the non-LTE Tk/CO_2 retrieval algorithm underestimates the radiation transfer simulations of the SABER 4.3 μm channel radiance measurements, which results in an overestimation of retrieved CO_2 vmr. Taking the northern hemisphere in Figure 6 as an example, the polar region is exposed to increasing periods and intensity of solar EUV flux as the seasons progress from winter to summer. Subsequently, the concentration of NO^+ increases from winter to summer, in response to the continual build up of the steady-state electron concentration (charge neutrality combined with NO^+ as the terminal E-region ion). The overestimated CO_2 concentration near high-latitude summer solstice (i.e., the southern hemisphere January 2003 SABER data and the northern hemisphere July 2002 SABER data) is coincident with the auroral oval latitude band due to the geometric effects of the geomagnetic field on the electron concentration.

11

Figures 7-9 summarize the results of the sensitivity study described above. Figure 7 shows zonal and daytime averaged NO^+ concentrations computed by the field-line interhemispheric plasma model (FLIP) for winter (January 24, 2003), summer (July 4, 2003), and equinox (September 22, 2003) seasons (Richards, 2002). The FLIP simulations clearly show an increase in high-latitude NO^+ as the seasons progress from winter to summer. There still remain large uncertainties in the E-region ion-neutral chemistry and $NO^+(v)$ kinetics (Mertens et al., 2007). Despite these uncertainties, we computed the contribution of $NO^+(v)$ to high-latitude summer SABER 4.3 μm limb radiance measurements, using the ion and neutral concentrations computed by the FLIP model and the methodology describe by Mertens et al. (2007).

Figure 8 shows broadband limb radiance simulations of the SABER 4.3 μm channel measurements for high-latitude daytime scans (i.e., solar zenith angles less than 85 degrees) on July 4, 2002. Figure 8 shows two sets of simulations: (1) CO_2 as the only emitter of 4.3 μm radiance, and (2) both CO_2 and NO^+ as emitters of 4.3 μm radiance. The simulations indicate that NO^+ contributes roughly 8% to the total SABER 4.3 μm emission at 135 km, 2% at 120 km, and less than 1% below 115 km. Enhancements of NO^+ due to geomagnetic activity will further increase the contribution of $NO^+(v)$ to the total 4.3 μm limb emission. $NO^+(v)$ emission contributes to a systematic bias in the SABER 4.3 μm channel forward model used in the non-LTE Tk/CO_2 retrieval, as previously described. The error in modeling the SABER 4.3 μm channel by not including $NO^+(v)$ 4.3 μm emission, as represented in Fig. 9, can bias the retrieved CO_2 vmr throughout the entire MLT region because the broadband 4.3 μm emission is strongly nonlinear in this region.

Figure 9 shows the SABER 4.3 μm limb radiance contribution functions for

a polar summer atmosphere with a solar zenith angle of 80 degrees. The tangent layer at 80 km contributes less 25% to the total limb radiance with non-negligible contributions coming from altitudes near 110 km, with smaller contributions from altitudes above 110 km. Tangent layers below 80 km contribute even less to the total limb radiance with non-negligible contributions also coming from altitudes near 110 km. The tangent layer at 100 km contributes about 25% to the total limb radiance with significant contributions coming from 120 km and non-negligible contributions coming from altitudes above 120 km.

The uncertainties in E-region ion-neutral chemistry and $NO^+(v)$ energetics prohibit an absolute estimate of the error in the SABER 4.3 μm channel forward model used in the non-LTE Tk/CO_2 retrieval, and the subsequent error in retrieved daytime CO_2 vmr. However, the results of the sensitivity studies presented Figures 7-9 combined with the positive-biased, step-function feature in the high-latitude summer SABER CO_2 vmr data located at the auroral oval region present a convincing argument that omission of $NO^+(v)$ 4.3 μm radiance in the SABER 4.3 μm forward model is a plausible explanation for the high-latitude summer season features in the SABER CO_2 vmr data.

Besides the anomalously large lower thermospheric CO_2 vmr in the high-latitude summer seasons described in detail above, the SABER CO_2 data appear to be quite reasonable. We evaluated the quality of the SABER CO_2 data in two ways: (1) by examining the effect of a SABER-CO_2 mean profile versus a TIME-GCM model profile on nighttime MLT Tk retrievals, and (2) by examining the effect of a SABER CO_2 vmr climatology versus the TIME-GCM CO_2 vmr climatology on comparisons of simulated nighttime 4.3 μm limb radiances with the corresponding SABER measurements. This valida-

13

tion study is described in the next subsection.

Figure 10 shows the SABER zonal mean CO_2 profile at $41°\,N$ for July 2002 (note: $41°\,N$ is outside the "anomalous" region in Figure 6). We choose to analyze the SABER-CO_2 mean profile at $41°\,N$ because there were six days of continuous sodium lidar MLT Tk measurements at Fort Collins, Colorado ($41°\,N$, $255°\,E$) (e.g., She et al., 2000). The lidar measurements will be used to assess the quality of the SABER-CO_2 data, as described below.

Figure 10 is a comparison of the SABER-CO_2 daytime mean profile, the TIME-GCM profile, and a rocket mass spectrometer measurement taken at mid-latitudes in the 1970s (see Wintersteiner et al., 1992). The horizontal line through the diamonds are the statistical fluctuations about the SABER monthly mean profile. The horizontal lines through the squares are $\pm$ the largest differences found between the SABER monthly mean profile and any single SABER observation during the month of July within 40-42°\,N. Figure 10 shows that the SABER-CO_2 mean profile deviates from the TIME-GCM model profile above 70 km. The SABER-model CO_2 deviations are significant above 90 km, i.e., greater than the largest difference between a single observed SABER-CO_2 profile and the corresponding monthly mean profile. Interestingly, the SABER-CO_2 mean profile is consistent with the rocket measurement made several decades ago (note: the rocket CO_2 profile has been scaled to reflect the current uniformly mixed value of ~ 365 ppmv).

Figure 11 shows the SABER-lidar MLT Tk comparisons for the six days of

14

sodium lidar measurements at Fort Collins, Colorado in July, 2002. We show all nighttime SABER Tk profiles in the latitude and longitude bands 35-45° N and 245-265° E, respectively. The SABER Tk profiles represent nearly instantaneous measurements at their respective geographical locations. The lidar Tk profiles are hourly averages, centered on the half-hour. We show lidar Tk profiles from the east-viewing beam (Lidar-E) and from the north viewing beam (Lidar-N) at three consecutive hourly intervals that bound the average SABER crossing time. We then average the SABER and lidar Tk profiles for each of the six days (mean profiles for 24 July shown in Figure 12). The mean Tk profiles are used to assess the quality of the SABER-CO_2 data, as described below. Unambiguous assessment of the SABER-CO_2 data is obtained from SABER-lidar Tk profiles that have the same vertical shape in the upper mesosphere and lower thermosphere, where differences in the rate of departure of CO_2 vmr from the uniformly mixed-value have a large effect on SABER-retrieved Tk. As a result, we use the SABER-lidar MLT Tk comparisons on 24 July to assess the quality of the SABER-CO_2 data.

The quality of the SABER-CO_2 mean profile in Figure 10 is assessed by comparing SABER nighttime Tk with sodium lidar measurements using the SABER-CO_2 mean profile versus the TIME-GCM model profile in the non-LTE Tk retrieval. Figure 12 shows a comparison of SABER-lidar mean nighttime Tk for July 24, 2002. Using the SABER-CO_2 mean profile in the nighttime non-LTE Tk retrieval rather than using the TIME-GCM model CO_2 profile reduced the differences between the SABER-lidar mean Tk by 5-7 K between 90 and 100 km. The improved SABER-lidar Tk comparisons in Figure 12 suggests that SABER-derived CO_2 data is a better representation of the true atmospheric MLT CO_2 abundance.

An alternative method of assessing the quality of the SABER CO_2 data is to compare simulated nighttime 4.3 μm limb radiances with the corresponding SABER measurements. Since the SABER nighttime 4.3 μm emission measurements are not used to derive any data products, the nighttime 4.3 μm measurements provide an independent observable to test the quality of the SABER-derived CO_2 vmr data. Monthly zonal mean SABER CO_2 vmr profiles were derived from the daytime retrievals. The nighttime SABER 4.3 μm channel radiance measurements were simulated using the non-LTE radiation transfer algorithm described by Mertens et al. (2007) and compared to the corresponding SABER measurements.

The simulated SABER nighttime 4.3 μm limb radiances were computed in two ways: (1) using the TIME-GCM climatological CO_2 vmr data, and (2) using the SABER-derived daytime monthly zonal mean CO_2 vmr data. We assume that the diurnal variation in CO_2 vmr is not significant below about 130 km. The results are shown in Figure 13 for July 2003. The profiles shown in Figure 13 are mean profiles averaged over all SABER measurement scans within each latitude band. The mean profiles in each latitude band were computed from hundreds of individual profiles. The black lines correspond to the SABER 4.3 μm limb radiance measurements. The blue lines correspond to simulated SABER 4.3 μm limb radiance using the TIME-GCM climatological CO_2 vmr data. The red lines correspond to simulated SABER 4.3 μm limb radiance using the SABER-derived monthly zonal (daytime) mean CO_2 vmr data. This figure indicates that the SABER-derived CO_2 vmr data significantly improve the simulated 4.3 μm limb radiances above about 90 km. We have done similar comparisons at all latitudes and for months representative of winter and summer seasons. The result of these comparisons is consistent

16

with the results presented in Figure 13. Thus, SABER-derived CO_2 vmr is a better representation of the true atmospheric CO_2 abundance compared to model simulations of CO_2 vmr.

4 Summary

We presented representative results of SABER Tk/CO_2 data from the version 1.06 dataset. The monthly zonal mean MLT Tk data clearly show the two-level structure of the mesopause altitude: the winter (high) mesopause altitude is 98 $\pm$ 1 km and the summer (low) mesopause altitude is 83 $\pm$ 1 km. Comparisons of polar summer MLT Tk during the 2002 summer MaCWAVE campaign between SABER and FS and lidar measurements are within 5-10 K below 85 km and between 90-95 km, respectively. The SABER summer mesopause altitude is lower than the FS measurements and Lübken climatology by 4-5 km, but consistent with mid-latitude lidar measurements of the summer mesopause altitude. The next version of the SABER dataset will incorporate isotopic CO_2 (ν_2) V-V exchange processes that may increase the SABER mesopause altitude and the lower mesospheric Tk.

The SABER CO_2 monthly zonal mean data are systematically lower than TIME-GCM model results above 70 km, consistent with previous analysis from infrared limb emission measurements. SABER-lidar MLT Tk differences are reduced by 5-7 K in the upper mesosphere and lower thermosphere using the SABER-derived CO_2 mean profile in the nighttime non-LTE Tk retrieval compared to using the TIME-GCM CO_2 mean profile in the non-LTE Tk retrieval. Moreover, differences in simulated nighttime SABER 4.3 μm channel radiances compared to the corresponding SABER measurements are signifi-

17

cantly reduced above 90 km by using SABER-derived mean CO_2 vmr data rather than TIME-GCM mean CO_2 vmr data. These two studies indicate a significant improvement in MLT CO_2 abundance made by SABER observations and analysis. However, SABER CO_2 appears to be overestimated at high-latitude summer seasons, possibly due to 4.3 μm emission from $NO^+(v)$ not accounted for in the non-LTE Tk/CO_2 retrieval algorithm. The high-latitude, high-bias in SABER CO_2 is noticeable at equinox and becomes much larger by summer solstice. Further investigations of this phenomena are currently underway.

Tk is an important input parameter for most of the other retrieval and photochemical algorithms used to generate the SABER routine and analysis data products. Accurate knowledge of both Tk and CO_2 are necessary to quantify the MLT radiative energy balance. As a result, high-quality Tk/CO_2 data are required to achieve the TIMED-SABER goal of advancing our understanding of the structure, energetics, and dynamics of the MLT region. The quality of the Tk/CO_2 data presented in this paper demonstrate the potential of the TIMED-SABER mission for making major advances in our understanding of the MLT region. Furthermore, the data presented in this paper provide a benchmark dataset for comparing the results of future updates to the SABER retrieval algorithms and data products.

References

Berger, U., and U. von Zahn, The two-level structure of the mesopause: A model study, J. Geophys. Res., 104, 22,083-22,093, 1999.

Kaufmann, M., O. A. Gusev, K. U. Grossmann, R. G. Roble, M. E. Hagan, C.

Hartsough, and A. A. Kutepov, The vertical and horizontal distribution of CO_2 densities in the upper mesosphere and lower thermosphere as measured by CRISTA, J. Geophys. Res., 107(D23), 8182, doi: 10.1029/2001JD000704, 2002.

Kutepov, A. A., A. G. Feofilov, B. T. Marshall, L. L. Gordley, W. D. Pesnell, R. A. Goldberg, and J. M. Russell III, SABER temperature observations in the summer polar mesosphere and lower thermosphere: Importance of accounting for the CO_2 ν_2 quanta V-V exchange, Geophys. Res. Lett., 33, L21809, doi:10.1029/2006GL026591, 2006.

López-Puertas, M., M. A. López-Valverde, R. R. Garcia, and R. G. Roble, A review of CO_2 abundances in the middle atmosphere, Geophysical Monograph 123, pp. 83-100, American Geophysical Union, Washington, DC, 2000.

Lübken, F. -J., Thermal structure of the Arctic summer mesosphere, J. Geophys. Res., 104, 9135-9149, 1999.

Mertens, C. J., M. G. Mlynczak, M. López-Puertas, P. P. Wintersteiner, R. H. Picard, J. R. Winick, L. L. Gordley, and J. M. Russell III, Retrieval of mesospheric and lower thermospheric kinetic temperature from measurements of CO_2 15 μm Earth limb emission under non-LTE conditions, Geophys. Res. Lett., 28, 1391-1394, 2001.

Mertens, C. J., M. G. Mlynczak, M. López-Puertas, P. P. Wintersteiner, R. H. Picard, J. R. Winick, L. L. Gordley, and J. M. Russell III, Retrieval of kinetic temperature and carbon dioxide abundance from non-local thermodynamic equilibrium limb emission measurements made by the SABER experiment on the TIMED satellite, Proceedings of SPIE, Remote Sensing of Clouds and the Atmosphere VII, Agia Pelagia, Crete, Greece, September 24-27, Vol. 4882, pp. 162-171, 2002.

Mertens, C. J., et al., SABER observations of mesospheric temperature

and comparisons with falling sphere measurements taken during the 2002 summer MaCWAVE campaign, Geophys. Res. Lett., 31, L03105, doi: 10.1029/2003GL018605, 2004.

Mertens, C. J., J. C. Mast, J. R. Winick, J. M. Russell III, M. G. Mlynczak, and D. S. Evans, Ionospheric E-region response to solar-geomagnetic storms observed by TIMED/SABER and application to IRI storm model development, Adv. Space Res., 39, 715-728, 2007.

Picone, J. M., A. E. Hedin, D. P. Drob, and A. C. Aikin, NRLMSIS-00 empirical model of the atmosphere: Statistical comparisons and scientific issues, J. Geophys. Res., 107(A12), 1468, doi:10.1029/2002JA009430, 2002.

Remsberg, E., G. Lingenfelser, V. L. Harvey, W. Grose, J. M. Russell III, M. Mlynczak, L. L. Gordley, and B. T. Marshall, On the verification of the quality of SABER temperature, geopotential height, and wind fields by comparison with Met Office assimilated analysis, J. Geophys. Res., 108(D20), 4628, doi: 10.1029/2003JD003720, 2003.

Remsberg, E., L. L. Gordley, B. T. Marshall, R. E. Thompson, J. Burton, P. Bhatt, V. L. Harvey, G. Lingenfelser, and M. Natarajan, The Nimbus 7 LIMS version 6 radiance conditioning and temperature retrieval methods and results, J. Quant. Spectrsc. Radiat. Transfer., 86(4), 395-424, 2004.

Richards, P. G., Ion and neutral density variations during ionospheric storms in September 1974: Comparison of measurement and models, J. Geophys. Res., 107(A11), 1361, doi:10.1029/2002JA00978, 2002.

Roble, R. G., Energetics of the mesosphere and thermosphere, The Upper Mesosphere and Lower Thermosphere: A Review of Experiment and Theory, American Geophysical Union Monograph 87, Wahsingdon, DC, 1995.

Russell, J. M. III, M. G. Mlynczak, L. L. Gordley, J. Tansock, and R. Esplin, An overview of the SABER experiment and preliminary calibration results,

Proceedings of the SPIE, 44th Annual Meeting, Denver, Colorado, July 18-23, Vol. 3756, pp. 277-288, 1999.

Schmidlin, F. -J., H. S. Lee, and W. Michael, The inflatable falling sphere: A technique for the accurate measurement of middle atmosphere temperatures, J. Geophys. Res., 96, 22,673-22,682, 1991.

Sharma, R. D., and P. P. Wintersteiner, Role of carbon dioxide in cooling planetary atmospheres, Geophys. Res. Lett., 17, 2201-2204, 1990.

She, C. Y., J. R. Yu, and H. Chen, Observed thermal structure of a midlatitude mesopause, Geophys. Res. Lett., 20(7), 567-570, 1993.

She, C. Y., J. R. Yu, D. A. Krueger, R. Roble, P. Keckhut, A. Hauchecorne, and M.-L. Chanin, Vertical structure of the midlatitude temperature from stratosphere to mesosphere (30-105 km), Geophys. Res. Lett., 22(4), 377-380, 1995.

She, C. Y., and U. von Zahn, Concept of a two-level mesopause: Support through new lidar observations, J. Geophys. Res., 103, 5855-5863, 1998.

She, C. Y., S. Chen, Z. Hu, J. Sherman, J. D. Vance, V. Vasoli, M. A. White, J. Yu, and D. A. Krueger, Eight-year climatology of nocturnal temperature and sodium density in the mesopause region (80 to 105 km) over Fort Collins, CO (41° N, 105° W), Geophys. Res. Lett., 27(20), 3289-3292, 2000.

von Zahn, U., J. Höffner, V. Eska, and M. Alpers, The mesopause altitude: Only two distinctive levels worldwide?, Geophys. Res. Lett., 23, 3231-3234, 1996.

Wintersteiner, P. P., R. H. Picard, R. D. Sharma, J. R. Winick, and R. A. Joseph, Line-by-line radiative excitation model for the non-equilibrium atmosphere: Application to CO_2 15-μm emission, J. Geophys. Res., 97, 18,083-18,117, 1992.

Zaragoza, G., M. López-Puertas, M. A. López-Valverde, and F. W. Tay-

lor, Global distribution of CO_2 in the upper mesosphere as derived from UARS/ISAMS measurements, J. Geophys. Res., 105(D15), 19,829-19,839, 2000.
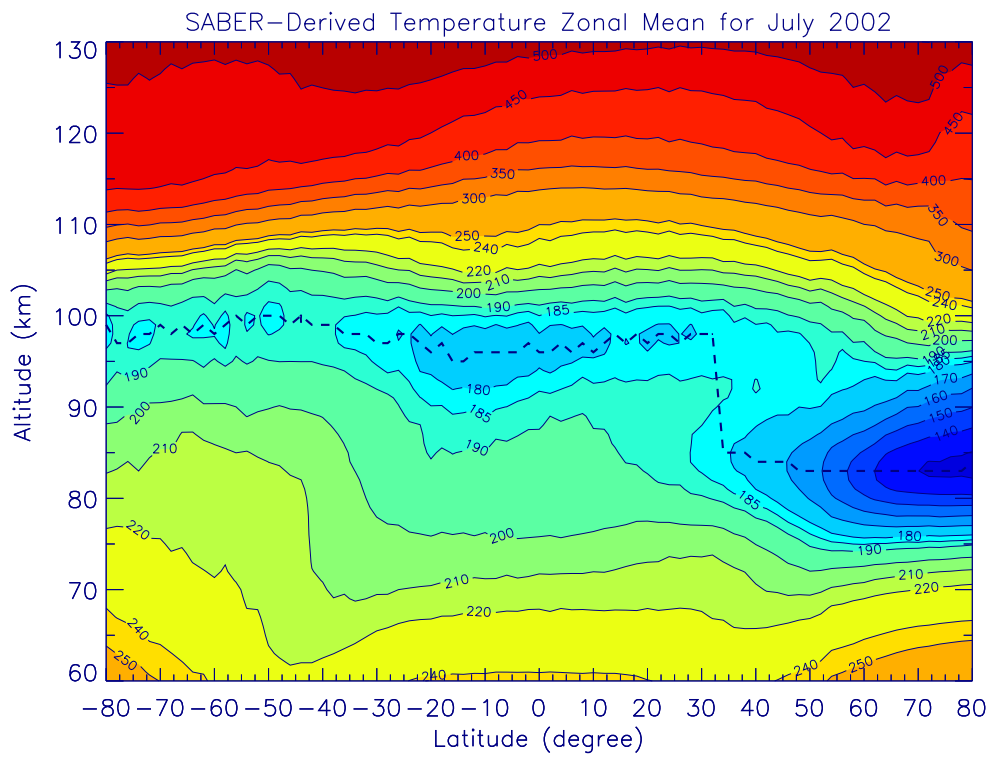
Fig. 1. Monthly zonal mean SABER temperatures for July 2002. The dotted line denotes the mesopause altitude.
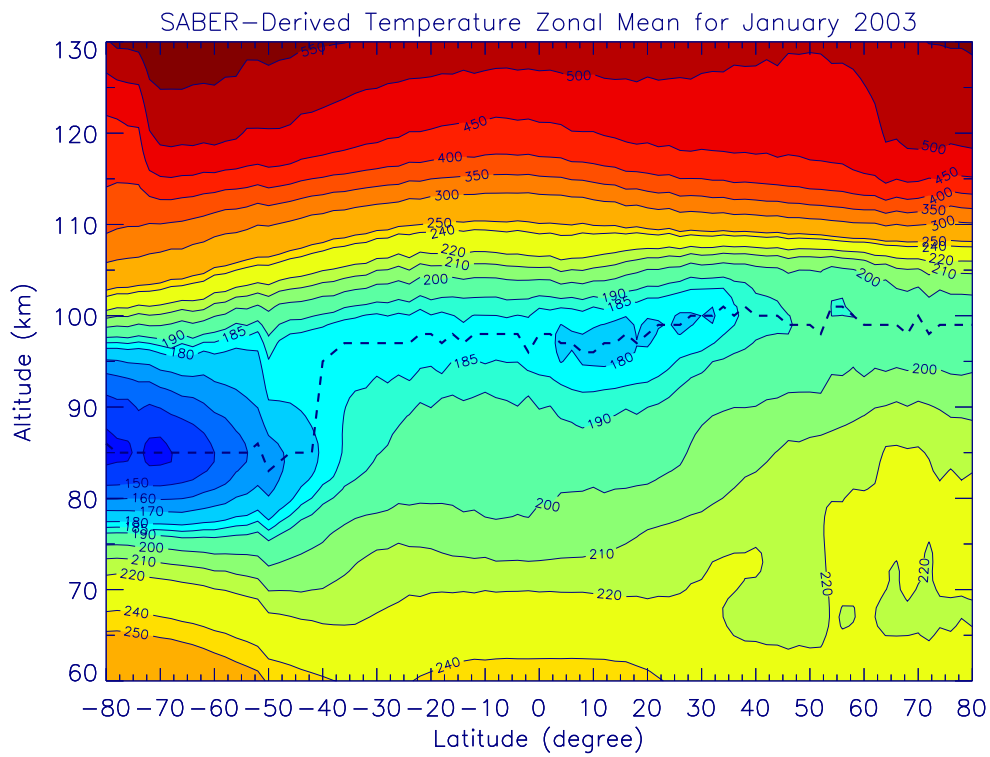
Fig. 2. Monthly zonal mean SABER temperatures for January 2003. The dotted line denotes the mesopause altitude.
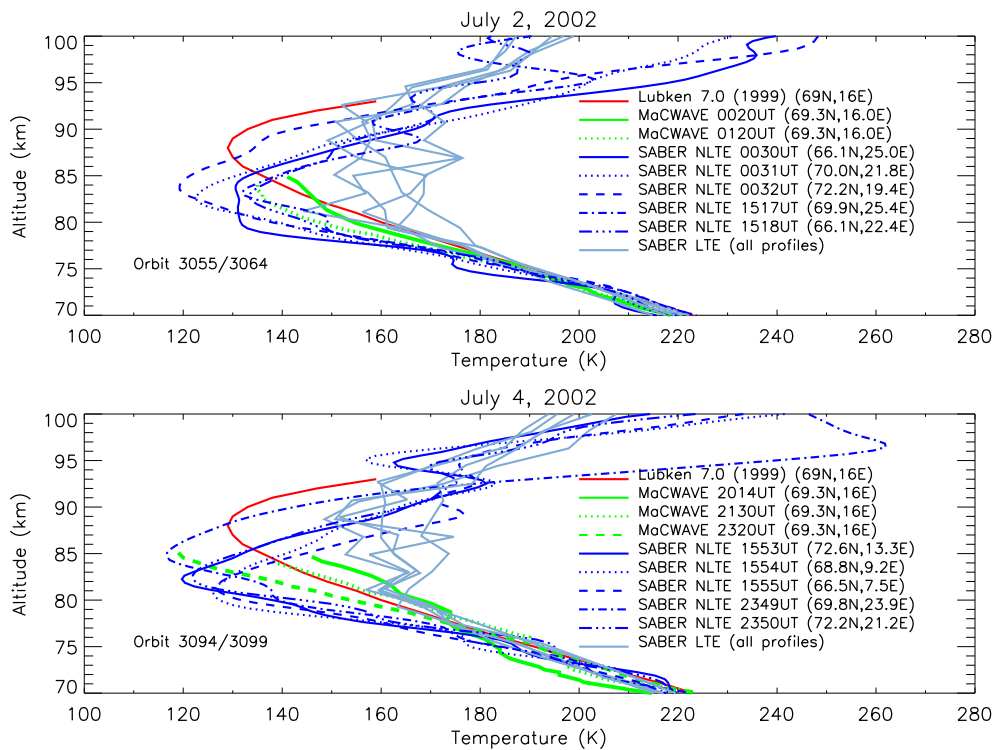
Fig. 3. SABER temperature comparisons with rocket falling sphere temperature measurements and the Lübken climatological profile during the summer 2002 MaCWAVE campaign.
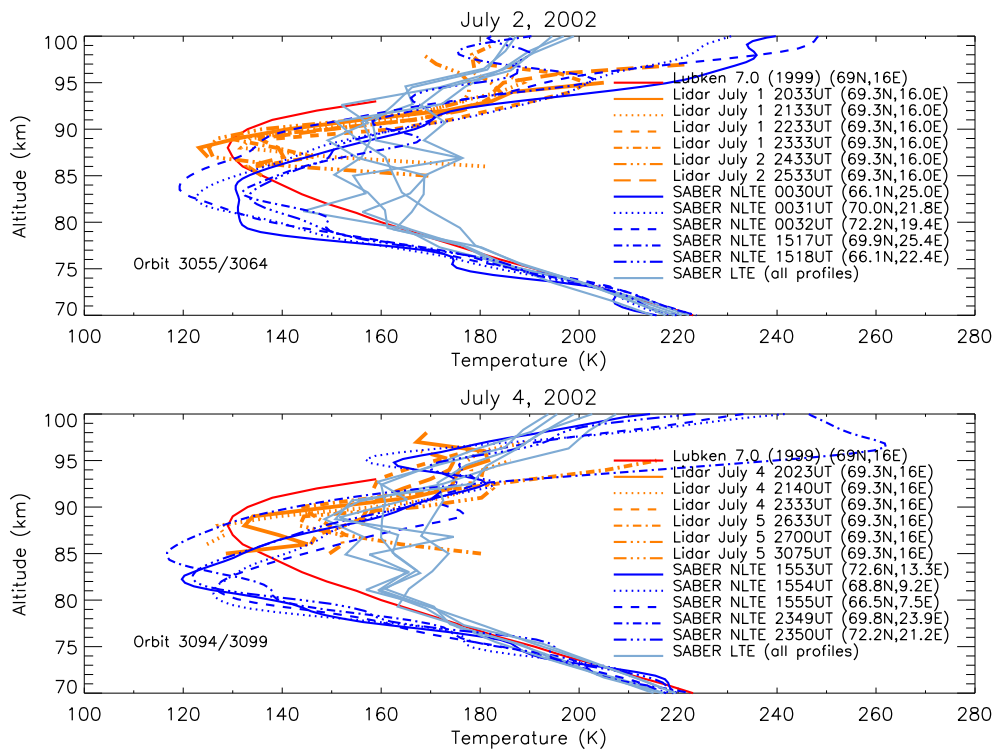
Fig. 4. SABER temperature comparisons with sodium lidar temperature measurements and the Lübken climatological profile during the summer 2002 MaCWAVE campaign.

26
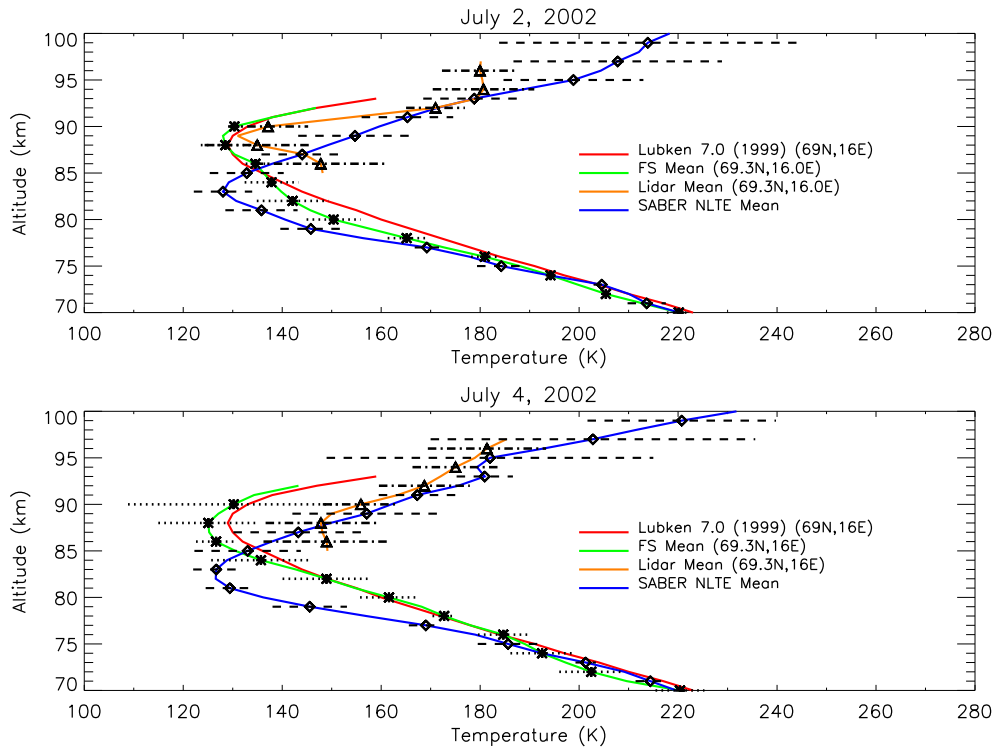
Fig. 5. Mean profiles of temperature measurements from SABER, rocket falling sphere, and sodium lidar observations during the summer 2002 MaCWAVE campaign. The horizontal lines are the statistical deviations with respect to the mean profiles. The Lübken climatological profile is also shown.
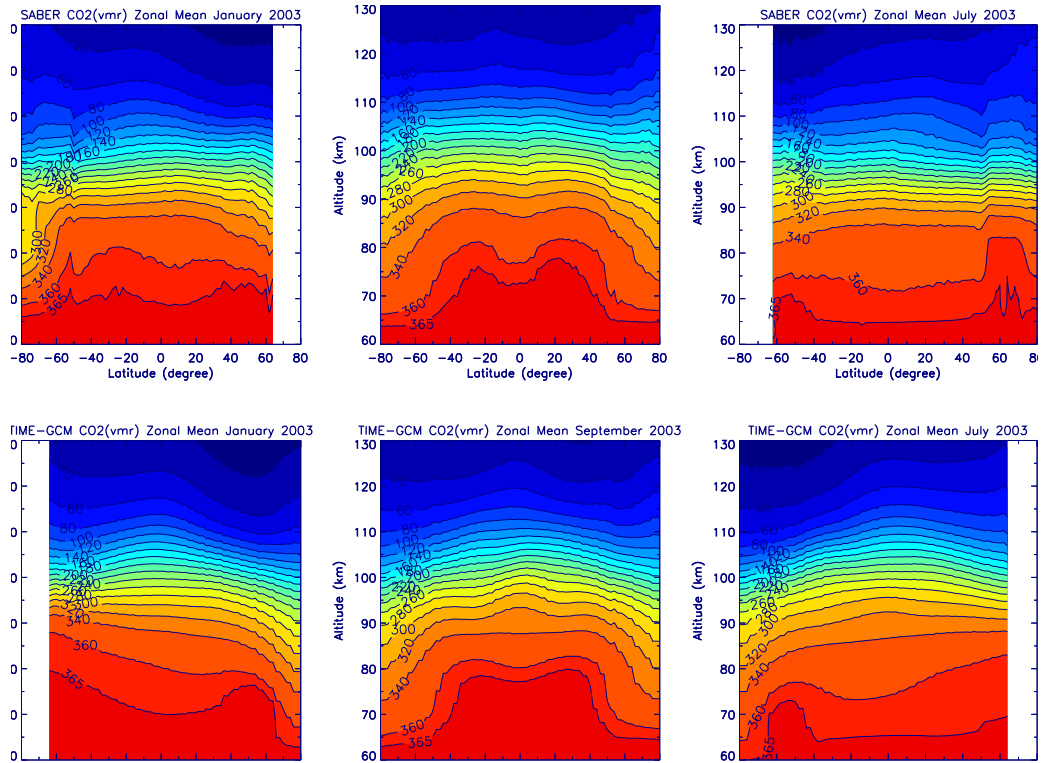
Fig. 6. Monthly zonal mean (daytime) CO_2 vmr data for northern hemisphere winter, equinox, and summer seasons. The top row is daytime SABER CO_2 vmr data and the bottom row is climatological daytime data computed from the TIME-GCM model.
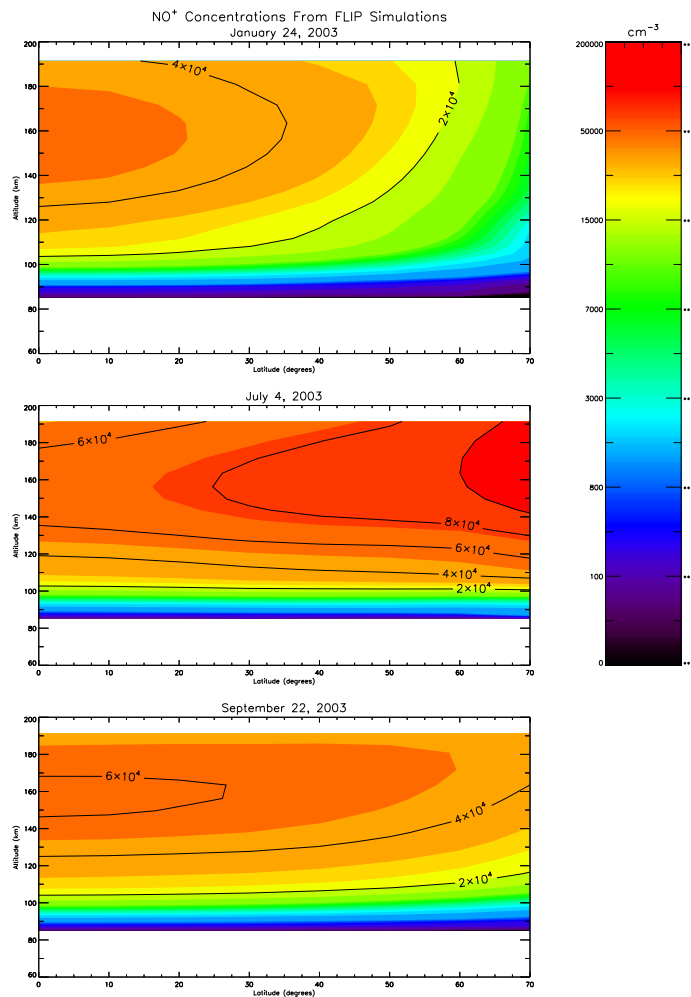
Fig. 7. Zonal and daytime averaged NO^+ concentrations computed by the FLIP model. Single-point geographic location flux tube simulations were run on a pre-defined global grid in order to obtain the zonal mean profiles. Hourly NO^+ output from FLIP were averaged over the daytime hours to compute the daytime mean.
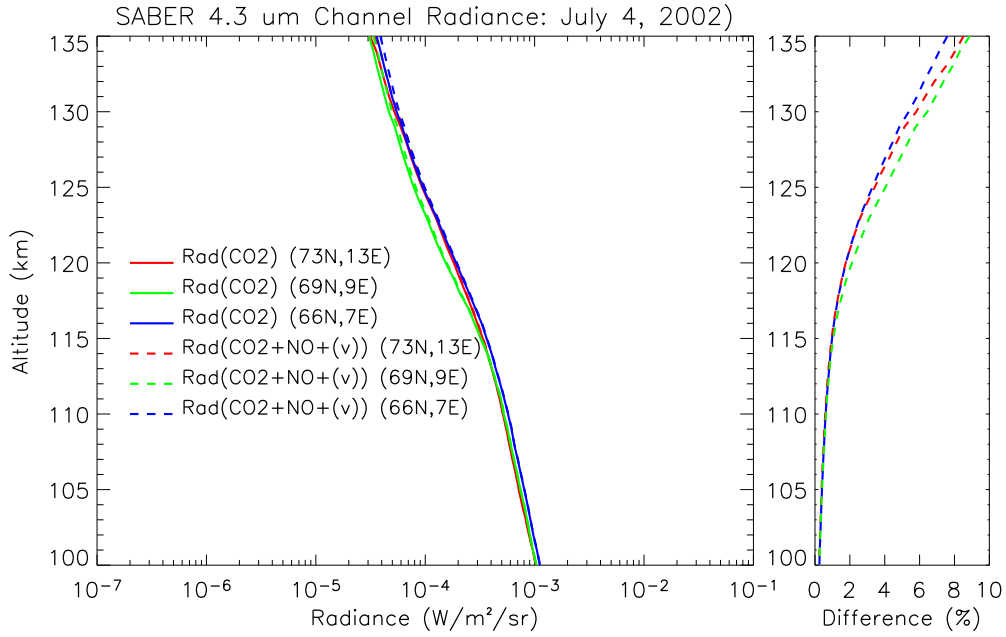
Fig. 8. Non-LTE radiation transfer simulations of the SABER 4.3 μm channel measurements for high-latitude scans on July 4, 2002. The solid lines are limb radiance simulations with CO_2 as the only emitter of 4.3 μm emission. The dashed lines are limb radiance simulations that include both CO_2 and NO^+ as emitters of 4.3 μm emission. The different colored lines denote different SABER meaurement scans. The right panel shows the percent contribution of $NO^+(v)$ 4.3 um emission to the total 4.3 μm limb radiance ($CO_2 + NO^+$).
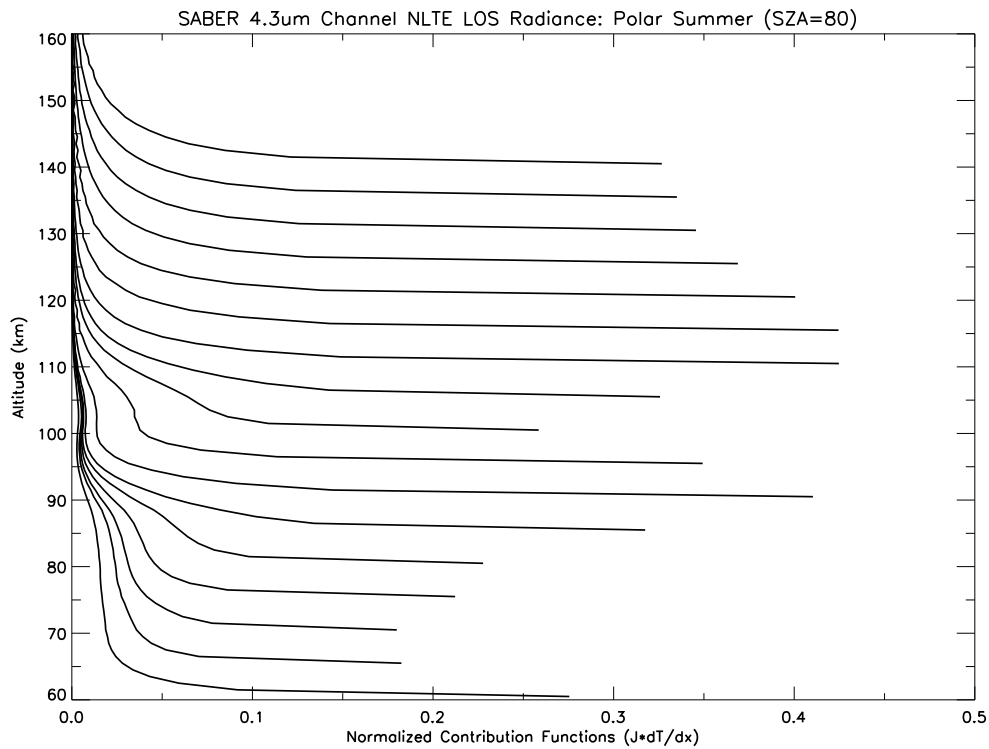
Fig. 9. Simulated SABER non-LTE 4.3 μm limb radiance contribution functions in the polar summer MLT region, with a solar zenith angle of 80 degrees. The contribution functions are normalized to the total 4.3 μm limb radiance. Each line represents the atmospheric layer contributions to the total limb radiance from different tangent heights. The contribution functions are shown for tangent heights from 60 km to 145 km in 5 km increments.
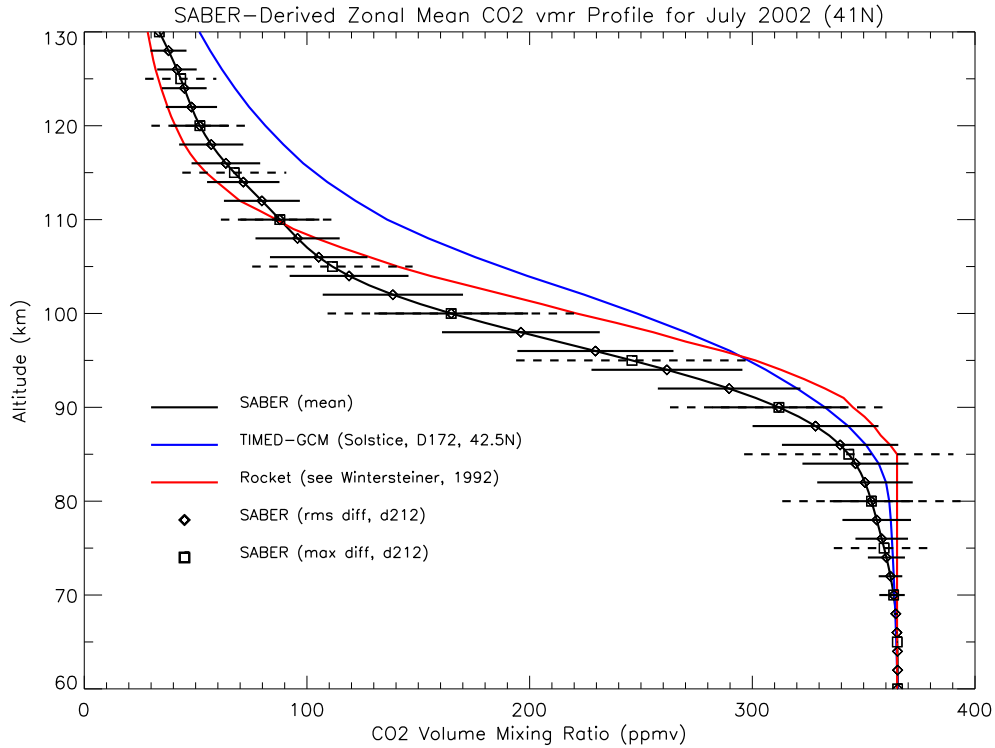
Fig. 10. Comparison of SABER CO_2 vmr profile with profiles computed by the TIME-GCM model and determined from a rocket-borne mass spectrometer measurement. The black line corresponds to a monthly zonal mean daytime SABER CO_2 vmr for July 2002, averaged between $40°$ N and $42°$ N. The horizontal lines through the diamonds are the statistical fluctuations about the mean profile. The horizontal lines through the squares are the maximum differences found between any single-event retrieved CO_2 vmr profile – in July 2002 between 40-$42°$ N – and the computed monthly mean profile. The blue and red lines correspond to the TIME-GCM simulation and the rocket measurement CO_2 vmr, respectively.
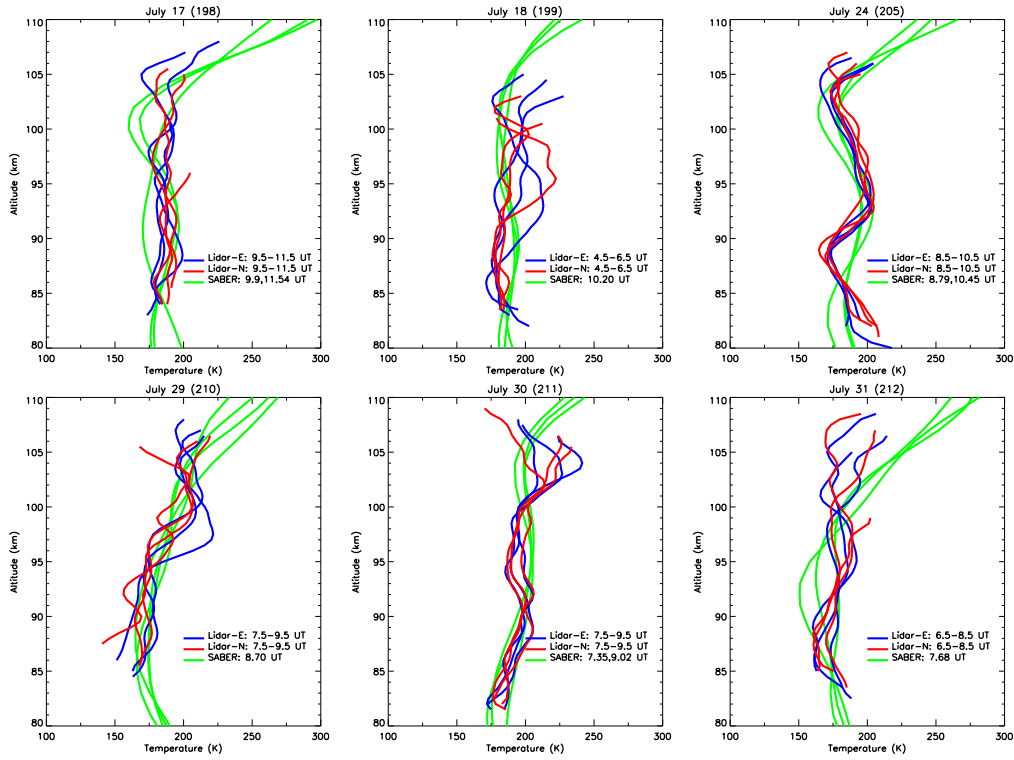
Fig. 11. Nighttime SABER and sodium lidar measurements of MLT Tk for six days in July, 2002. The lidar measurements were taken at Fort Collins, CO, located at 41° N, 255 ° E. The blue lines are lidar measurements from the east-viewing beam. The red lines are lidar measurements from the north-viewing beam. The lidar Tk profiles represent hourly averages, centered on the half-hour. The green lines are SABER Tk profiles between 35-45° N and 245-265° E.
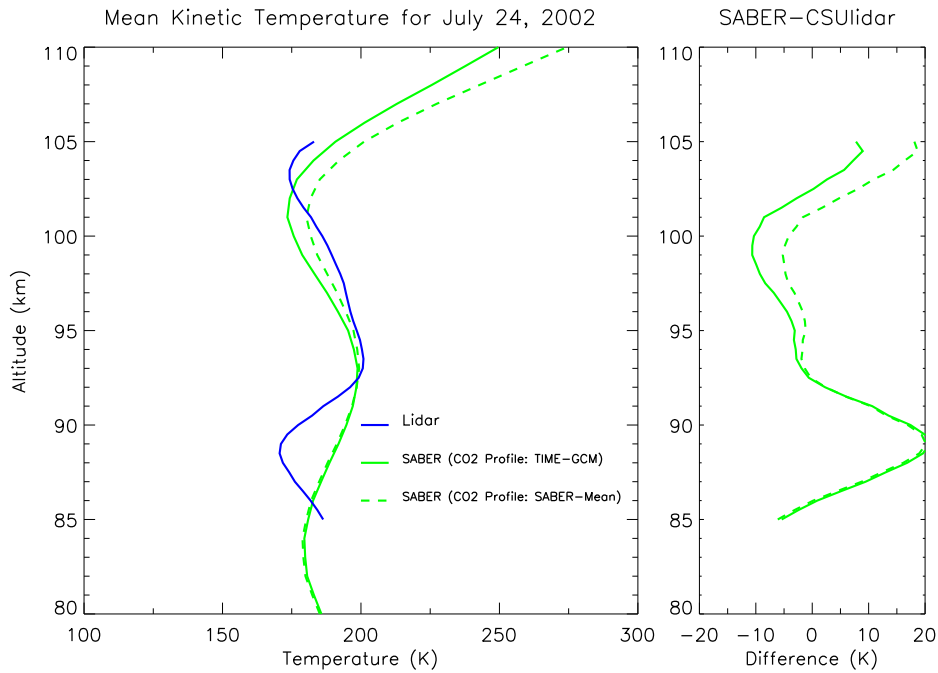
Fig. 12. Comparison of the mean SABER nighttime Tk profile for July 24, 2002 with the mean lidar Tk profile. The SABER and lidar mean profiles were computed from the single measurement profiles shown in Figure 11. The solid green line corresponds to nominal SABER nighttime Tk retrieved using the TIME-GCM CO_2 vmr profile (i.e., the blue line in Figure 10). The dashed green line corresponds to SABER nighttime Tk retrieved using a SABER-derived mean CO_2 vmr profile (i.e., the black line in Figure 10).
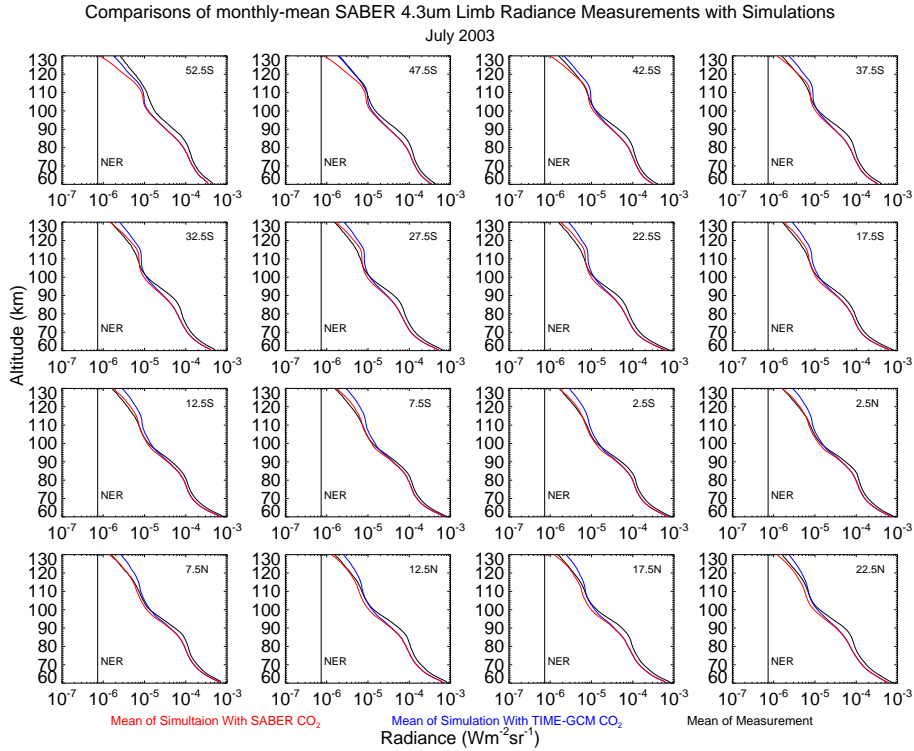
Fig. 13. Comparison of monthly mean SABER nighttime 4.3 μm limb radiance measurements with simulated SABER 4.3 μm limb radiances for July 2003. The black lines correspond to the SABER 4.3 μm limb radiance measurements. The blue lines correspond to simulated SABER nighttime 4.3 μm limb radiance using TIME-GCM CO_2 vmr data. The red lines correspond to simulated SABER nighttime 4.3 μm limb radiance using SABER-derived monthly (daytime) mean CO_2 vmr data. Each latitude band respresents an average of hundreds of SABER measurement scans.